

COMMUNICATION

[View Article Online](#)
[View Journal](#) | [View Issue](#)

Cite this: *Polym. Chem.*, 2023, **14**, 2670

Received 11th May 2023,
Accepted 19th May 2023

DOI: 10.1039/d3py00517h

rsc.li/polymers

UV-curable polyurethane-acrylate hybrids made by a prepolymer-free process and free-standing polymer–metal oxide films made in a wholly water-based UV curing process†

Roshan F. Dsouza‡ and Anbanandam Parthiban *

Acrylates are widely used for UV curing to coat substrates and to form shaped articles. Of late, UV curing has gained prominence in 3D printing and additive manufacturing technologies. The process described here helps in enhancing the concentration of acrylates at specified locations of the polymer chain, is free from volatile components, and is entirely based on water.

The UV curing of acrylates and hybrid polyurethane acrylates has historically been used for protective coatings,^{1,2} in photolithography,³ and in dentistry.⁴ Polyurethane-acrylates are also used as adhesives.^{5,6} Recently, their applications have been reported in biomedicines,⁷ roll-to-roll printing of adhesive layers for transferring complex microstructures⁸ and oil–water separation technologies.⁹ Over the years the UV curing process has evolved and expanded into emerging areas like additive manufacturing.^{10–12} Conventionally, aqueous polyurethane dispersions^{13,14} or reactive diluents are used in UV curing applications.¹ In spite of its many attractive features, there are many concerns about the UV curing process. For example, the reactive diluents used in the curing process pose issues of toxicity, volatility, and irritation to the eyes and skin.¹⁵ The aqueous polyurethane dispersion process is complicated since it involves an inversion step of transferring the components from an organic solvent to the aqueous medium. This process not only introduces residual solvents but also requires volatile organic bases like triethyl amine or gaseous bases like ammonia to facilitate dispersion in water by neutralizing acidic functionalities present in the prepolymer.¹ In addition, the introduction of the acrylate functionality that is essential for the curing process is either limited to chain ends or

requires sensitive multifunctional reagents like hydroxy acrylates to increase its concentration. In order to achieve an optimum performance of cured substrates in terms of hardness, and resistance to scratch, solvent, and stain, a higher concentration of acrylate functionalities is needed.^{1,16} As the process offers enormous promise in some emerging areas like the photocurable direct-ink-writing method,⁹ significant improvements are needed in the development of photocurable components.

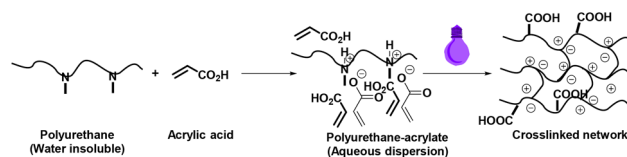
First and foremost, unlike the conventional photocurable components used currently, the number of crosslinking sites needs to be increased and preferably its location predetermined and specified in the polymer chain. Handling of components should be simplified and equally importantly, the number of components should be minimized. By keeping these aspects in mind, we developed a UV curing approach that fundamentally makes use of the acid–base interaction between a urethane-based polymer consisting of the tertiary amine functionality and an acidic photocurable monomer like acrylic acid as shown in Scheme 1.

The proposed approach has several advantages as compared to the conventional process. The prepolymer process as practiced conventionally actually limits the molecular weight of polyurethane due to two major reasons. One is that, because of the end-capping mechanism, the molecular weight is inherently limited. Secondly, since the dilution of end groups becomes prominent with increasing molecular weight, the molecular weight needs to be kept low. This restriction on the molecular weight of the prepolymer also prevents the use

*Institute of Sustainability for Chemicals Energy and Environment (ISCE²), Agency for Science Technology and Research (A*STAR), 1, Pesek Road, Jurong Island, Singapore 627833. E-mail: a_parthiban@isce2.a-star.edu.sg*

†Electronic supplementary information (ESI) available: Detailed synthetic procedures, ¹H-NMR spectra of polymers. See DOI: <https://doi.org/10.1039/d3py00517h>

‡Present address: Department of Chemistry, St Aloysius College (Autonomous), Mangaluru 575003, India.



Scheme 1 A wholly water-based UV curing process with variable photocurable units at specified locations.

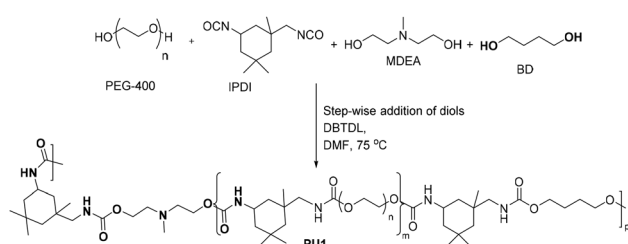
of multiple components. Thus, one is hindered from making use of the immense diversity of material properties that polyurethane chemistry offers. The proposed approach overcomes these limitations in a facile manner. It can be visualized that the proposed approach makes it possible to use any kind of polymer backbone that enables this acid–base interaction, thereby enhancing the property variation of UV-cured substrates. As acid–base interactions are fairly strong, no volatile reactant or reagent is eliminated into the atmosphere in the proposed process. To fine-tune the properties of cured substrates, it is possible to use other curable components. In addition, functional components can be included in the curing process to obtain cured coated substrates as well as free-standing functional films.

Polymer–metal oxide hybrid films have wide applications, and the application area is determined by the nature of the polymer and the type of metal oxide. Polymer–metal oxide hybrid materials have been used in catalysis,¹⁷ in electronic applications as thin film transistors,¹⁸ in solar cells,^{19–22} as memristors,²³ in flexible electronic devices,²⁴ in semi-conductors for wearable electronics,²⁵ as hardeners,¹⁶ as barrier films,²⁶ as nanocomposites,^{27,28} in corrosion resistant coatings^{29,30} and in gas separation membranes.^{31–35} Hence, we chose to demonstrate the wholly water-based, prepolymer-free UV curing process for preparing poly(urethane-acrylate-TiO₂) (PU-AA-TiO₂) and poly(urethane-acrylate-SiO₂) (PU-AA-SiO₂) hybrid films, as TiO₂ and SiO₂ are widely used in coating and other applications.

The tertiary amine-containing polyurethane was prepared as shown in Scheme 2 by stepwise addition of monomers.

Polyethylene glycol 400 (PEG 400) was reacted with isophoron diisocyanate (IPDI) by heating in *N,N*-dimethyl formamide (DMF) in the presence of the catalyst, dibutyltin dilaurate (DBTDL), followed by reacting with *N*-methyl diaethanolamine (MDEA) and subsequently with 1,4-butanediol (BD). At the end of the reaction, the polymer solution was precipitated in water to isolate PU1.

PU1 was characterized by FT-IR and ¹H-NMR spectroscopic analysis to confirm its chemical structure. PU1 was also characterized by gel permeation chromatography and thermogravimetric analysis. The number average molecular weight (av. *M_n*) of PU 1 using THF as the eluent was 10 100 Daltons with a polydispersity, *D*, of 1.8. Fig. S1† shows the ¹H-NMR spectrum of PU1.



Scheme 2 Preparation of the "basic" polyurethane, PU1.

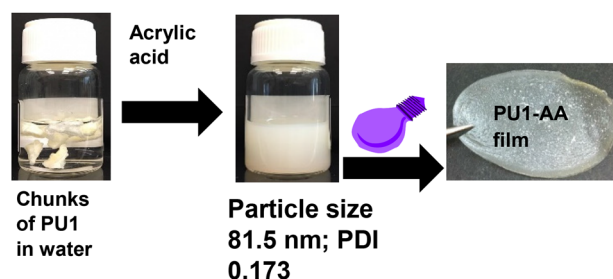


Fig. 1 Appearance and characteristics of aqueous dispersions and the cured film.

In the next step, PU1 was suspended in deionized water, acrylic acid was added and the solution was then stirred under ambient conditions for 6 h to provide a solid content of 10 wt%. As shown in Fig. 1, initially, chunks of PU1, some floating and others immersed in deionized water, were visible. Subsequently, the chunks of PU1 were smoothly dispersed after adding acrylic acid (AA) and upon stirring under ambient conditions. Dynamic light scattering analysis indicated that the particles formed were unimodal with a PDI of 0.173 (Fig. 2).

After mixing with the photoinitiator, 2-hydroxy-4'-(2-hydroxyethoxy)-2-methylpropiophenone, the aqueous dispersion was cured under UV using a bench top UV lamp (λ_{max} 36 nm) (a UV gel nail polish dryer) under a nitrogen atmosphere to yield a free-standing film. The FT-IR analysis of cured PU1-AA indicated the broadening of the signal in the carbonyl region as compared to PU1 as shown in Fig. 3 due to the additional

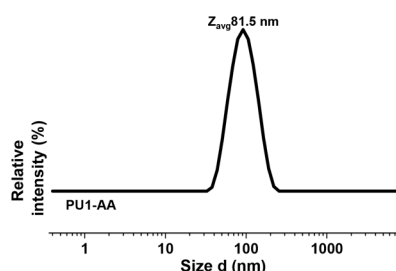


Fig. 2 Particle size of the PU1-AA aqueous dispersion.

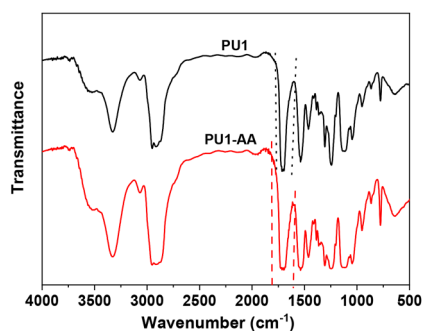


Fig. 3 FT-IR analysis of PU1 and PU1-AA.

absorption in the carbonyl region caused by the introduction of acrylates. The absence of signals corresponding to the C=C bond in Fig. 3 indicated that the curing is nearly quantitative.

In a separate experiment, to the dispersion of PU1 and AA in deionized water, TiO_2 and SiO_2 were added in separate vials followed by addition of the photoinitiator. After mixing well by stirring under ambient conditions, the dispersions were transferred to a Teflon disc and cured using a bench-top UV lamp under a nitrogen atmosphere for an hour. At the end of the curing reaction, the cured film was removed from the Teflon disc and rinsed with deionized water and then dried under ambient conditions. A control experiment was conducted in which a similar aqueous medium consisting of AA and TiO_2 was used without PU1 and then cured as before after adding the photoinitiator. Unlike the TiO_2 cured with PU1, as shown in Fig. 4, no film was obtained in the control experiment.

The stability of the PU1-AA- TiO_2 film was tested by heating it in deionized water at 90 °C for 12 h. As shown in Fig. 4, the film remained intact after hot water treatment. No aggregation was noticed in the heat-treated film and the metal oxide remained well dispersed similar to the untreated, cured hybrid film. But for the shrinkage induced by heat treatment, no separation of inorganic oxides was noticed as the water used for heating the film remained clear, thereby indicating the completeness of the curing and the strong interactions that prevailed among the hybrid components. SiO_2 dispersed in PU1-AA was similarly cured to obtain a free-standing film of PU1-AA- SiO_2 .

SEM analysis of PU1-AA-metal oxide hybrid films was conducted as shown in Fig. 5 and indicated that the films were smooth and homogeneous.

Thermogravimetric analysis (TGA) confirmed the presence of metal oxides in the hybrid films. As expected for an ali-

phatic polymer, no residue remained after heating PU1-AA under a nitrogen atmosphere at 600 °C due to the complete degradation of PU1-AA.

Residues were observed in both PU1-AA- TiO_2 and PU1-AA- SiO_2 , after heating up to 800 °C under a nitrogen atmosphere. Fig. 6 shows the TGA of hybrid polymer PU1-AA and polymer-metal oxide hybrids. The shape of the thermograms also indicated the absence of any volatiles in the cured films. The thermal stability of the polymer-metal oxide hybrid film was better as the thermogram was stable up to the degradation of the polymer chain that started at 265 °C. The metal oxide-free polymer film PU1-AA started to degrade at 180 °C. The low thermal stability is due to the aliphatic nature of the polymers. The improved thermal stability of the polymer-metal oxide hybrid film is likely due to the fact that the metal oxide in the hybrid film acted like a heat sink and protected the organic polymer initially.

Acid-base interactions were utilized to overcome some of the challenges prevailing in the acrylate-based UV curing process. This not only enabled an increase in the concentration of the photocurable acrylate functionality but also helped to anchor the photocurable functionality at pre-determined positions through the interaction of the carboxylic acid functionality with the tertiary amino group. In addition, the end-capping approach commonly employed in the conventional UV curing of urethane-acrylate hybrid systems was entirely avoided. The tertiary amine-containing polymer was smoothly dispersed in deionized water after adding acrylic acid and stirring under ambient conditions. DLS studies indicated the formation of uniform monodisperse particles. Hybrid poly(acrylate-urethane) films and polymer-metal oxide hybrid films were obtained by a UV curing process that is free from volatile solvents, reagents and is entirely based on water. Hybrid polymer-metal oxide films were found to be stable after curing as shown by hot water treatment. In the absence of "basic" polyurethane, the UV cured AA- TiO_2 system did not form a free-standing hybrid film of polymer-metal oxide. This approach has been extended for making free-standing coloured and colourless polymer films, transparent and

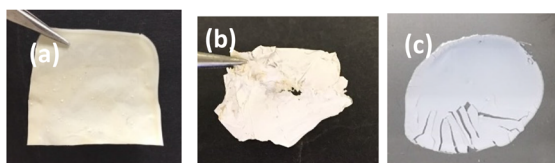


Fig. 4 The PU1-AA- TiO_2 film (a) after curing and (b) after being heated in water at 90 °C for 12 h, and (c) the solid formed by the aqueous dispersion of AA- TiO_2 after UV curing.

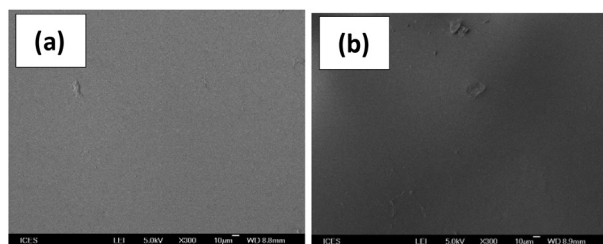


Fig. 5 SEM images of (a) PU1-AA- TiO_2 and (b) PU1-AA- SiO_2 films.

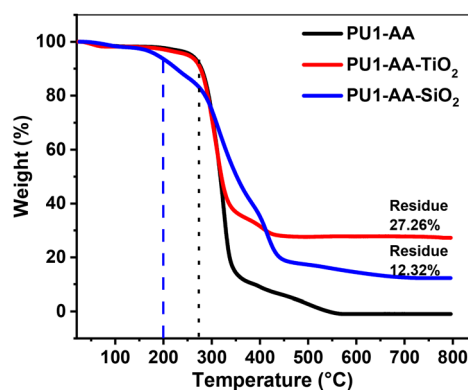


Fig. 6 The thermogravimetric analysis of polymer hybrids and polymer-metal oxide hybrids.



opaque coated substrates of metals and glass and photocurable inks. These results will be reported shortly. Cured substrates bearing an ammonium functionality have been reported to be useful as anti-fog coatings.³⁶

With growing concerns about emissions from solvents and residual volatiles from coatings^{37–39} and the fact that UV curing is gaining prominence in additive manufacturing,^{40–42} the process reported here holds much promise across a wide range of applications. The polymer–metal oxide hybrid films prepared here can be extended to prepare corrosion-resistant coated substrates, hybrid membranes and functional films using other metal oxides. The acid–base interactions can be fundamentally extended to many polymeric systems, thereby broadening the substrate scope and thus offering tremendous possibilities in the areas of additive manufacturing, coating and 3D printing. The availability of both the wide range of raw materials for making polyurethanes and the extensive literature on the structure–property understanding of polyurethanes makes it possible to prepare non-volatile, photocurable systems. Importantly, this development potentially shifts the operation from industrial manufacturing facilities to the domain of a do-it-yourself (DIY) kind of activity.

Author contributions

RFD contributed formal analysis, investigation, methodology and validation. AP contributed conceptualization, formal analysis, funding acquisition, methodology, project administration, supervision and writing the original draft.

Conflicts of interest

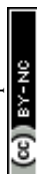
There are no conflicts to declare.

Acknowledgements

This work was funded by the Agency for Science, Technology and Research (A*STAR), Singapore under Environmentally Friendly Specialty Products Programme (Grant No.: 1528000045).

References

- 1 R. Tennebroek, I. v. d.-H. van Casteren, R. Swaans, S. v. d. Slot, P. J. M. Stals, B. Tuijelaars and C. Koning, *Polym. Int.*, 2019, **68**, 832.
- 2 S.-Y. Park, J. Cheon, B. Y. Jeong, D. H. Lee, P. Huh and J. H. Chun, *Mol. Cryst. Liq. Cryst.*, 2020, **706**, 129.
- 3 H. Molavi, A. Shojaei and S. A. Mousavi, *Polymer*, 2018, **149**, 178.
- 4 H. Gong, X. Guo, D. Cao, P. Gao, D. Feng, X. Zhang, Z. Shi, Y. Zhang, S. Zhu and Z. Cui, *J. Mater. Chem. B*, 2019, **7**, 744.
- 5 H. Xiang, X. Wang, G. Lin, L. Xi, Y. Yang, D. Lei, H. Dong, J. Su, Y. Cui and X. Liu, *Polymers*, 2017, **9**, 552.
- 6 J. Cheon, S.-Y. Park, B. Y. Jeong and J. H. Chun, *Mol. Cryst. Liq. Cryst.*, 2020, **706**, 62.
- 7 S. Balcioglu, S. A. A. Noma, A. Ulu, M. G.-K. Tunc, O. Ozhan, S. Koytepe, H. Parlakpinar, N. Vardi, M. C. Colak and B. Ates, *ACS Appl. Mater. Interfaces*, 2022, **14**, 41819.
- 8 J.-K. Kim, N.-K. Subbaiah, Y. Wu, J. Ko, A. Shiva and M. Sitti, *Adv. Mater.*, 2023, **35**, 2207257.
- 9 H. Chen, J. Yang, J. Su and Y. Cui, *Sep. Purif. Technol.*, 2022, **303**, 122239.
- 10 G.-R. Sabat, L. A. Granda and S. Medel, *Mater. Adv.*, 2022, **3**, 5118.
- 11 K. Chen, X. Kuang, V. Li, G. Kang and H. J. Qi, *Soft Matter*, 2018, **14**, 1879.
- 12 G. Taormina, C. Sciancalepore, M. Messori and F. Bondioli, *J. Appl. Biomater. Biomech.*, 2018, **16**, 151.
- 13 F. Wang, J. Q. Hu and W. P. Tu, *Prog. Org. Coat.*, 2008, **62**, 245.
- 14 M. Tielemans, P. Roose, C. Ngo, R. Lazzaroni and P. Leclerc, *Prog. Org. Coat.*, 2012, **75**, 560.
- 15 M. Kury, K. Ehrmann, G. A. Harakály, C. Gorsche and R. Liska, *J. Polym. Sci.*, 2021, **59**, 2154.
- 16 J. Fu, H. Yu, L. Wang, R. Liang, C. Zhang and M. Jin, *Prog. Org. Coat.*, 2021, **153**, 106121.
- 17 A. R. Wassela, M. E. El-Naggar and K. Shoueir, *J. Environ. Chem. Engg.*, 2020, **8**, 104175.
- 18 J. W. Jeong, H. S. Hwang, D. Choi, B. C. Ma, J. Jung and M. Chang, *Micromachines*, 2020, **11**, 264.
- 19 J. Boucle, S. Chyla, M. S. P. Shaffer, J. R. Durrant, D. D. C. Bradley and J. Nelson, *Adv. Funct. Mater.*, 2008, **18**, 622.
- 20 P. Atienzar, T. Ishwara, M. Horie, J. R. Durrant and J. Nelson, *J. Mater. Chem.*, 2009, **19**, 5377.
- 21 J. Bouclé, P. Ravirajana and J. Nelson, *J. Mater. Chem.*, 2007, **17**, 3141.
- 22 J. Qi, J. Chen, W. Meng, X. Wu, C. Liu, W. Yu and M. Wang, *Synth. Met.*, 2016, **222**, 42.
- 23 S. Stathopoulos, I. Tzouvadaki and T. Prodromakis, *Sci. Rep.*, 2020, **10**, 21130.
- 24 S. Kumagai, H. Murakami, K. Tsuzuku, T. Makita, C. Mitsui, T. Okamoto, S. Watanabe and J. Takeya, *Org. Electron.*, 2017, **48**, 127.
- 25 S. Pletincx, K. Marcoen, L. Trotochaud, L.-L. Fockaert, J. M. C. Mol, A. R. Head, O. Karslioglu, H. Bluhm, H. Terryn and T. Haufman, *Sci. Rep.*, 2017, **7**, 13341.
- 26 J. W. Na, H. J. Kim, S. Hong and H. J. Kim, *ACS Appl. Mater. Interfaces*, 2018, **10**, 37207.
- 27 A. Madhi, B. S. Hadavand and A. Amoozadeh, *J. Compos. Mater.*, 2018, **52**, 2973.
- 28 S. Lv, W. Zhou, H. Miao and W. Shi, *Prog. Org. Coat.*, 2009, **65**, 450.
- 29 E. Kabaoglu, F. Karabork, D. B. Kayan and A. Akdemir, *J. Compos. Mater.*, 2023, **57**, 451.
- 30 H. Wang, J. Xu, H. Wang, X. Cheng, S. Wang and Z. Du, *Prog. Org. Coat.*, 2022, **167**, 106897.
- 31 M. Sandru, E. M. Sandru, W. F. Ingram, J. Deng, P. M. Stenstad, L. Deng and R. J. Spontak, *Science*, 2022, **376**, 90.



- 32 C. Knebel, *Nat. Nanotechnol.*, 2022, **17**, 911.
- 33 S. Boncel, W. Kaszuwara, A. Kolanowska, S. D. Kolev, A. Rybak and A. Rybak, *RSC Adv.*, 2022, **12**, 13367.
- 34 K. Baskaran, M. Ali, K. Gingrich, D. L. Porter, S. Chong, B. J. Riley, C. W. Peak, S. E. Naleway, I. Zharov and K. Carlson, *Microporous Mesoporous Mater.*, 2022, **336**, 111874.
- 35 K. Kuraoka and R. Yamamoto, *J. Sol-Gel Sci. Technol.*, 2022, **104**, 470.
- 36 J. W. Hong, H. K. Cheon, S. H. Kim, K. H. Hwang and H. K. Kim, *Prog. Org. Coat.*, 2017, **110**, 122.
- 37 C. E. Stockwell, M. M. Coggon, G. I. Gkatzelis, J. Ortega, B. C. McDonald, J. Peischl, K. Aikin, J. B. Gilman, M. Trainer and C. Warneke, *Atmos. Chem. Phys.*, 2021, **21**, 6005.
- 38 V. Kultun, S. Thepanondh, N. Pinthong, J. Keawboonchu and M. Robson, *Atmosphere*, 2022, **13**, 1515.
- 39 R.-T. Gruener, P. E. Rajan, L. D. Dugan, M. E. Bier, A. L. Robinson and A. A. Presto, *Environ. Sci. Technol.*, 2022, **56**, 11236.
- 40 M. Mahmoudi, C. Wang, S. Moreno, S. R. Burlison, D. Alatalo, F. Hassanipour, S. E. Smith, M. Naraghi and M. M. Jolandan, *ACS Appl. Mater. Interfaces*, 2020, **12**, 31984.
- 41 J. M. Chacon, M. A. Caminero, E.-G. Plaza and P. J. Núñez, *Mater. Des.*, 2017, **124**, 143.
- 42 C. McIlroy and P. D. Olmsted, *Polymer*, 2017, **123**, 376.

